Estimating the Sensitivity of Radiative Impacts of Shallow, Broken Marine Clouds to Boundary Layer Aerosol Size Distribution Parameter Uncertainties for Evaluation of Satellite Retrieval Requirements

ANN M. FRIDLIND AND ANDREW S. ACKERMAN

NASA Goddard Institute for Space Studies, New York, New York

(Manuscript received 18 August 2010, in final form 18 November 2010)

ABSTRACT

A proposed objective of the planned Aerosol–Cloud–Ecosystem (ACE) satellite mission is to provide constraints on climate model representation of aerosol effects on clouds by retrieving profiles of aerosol number concentration, effective variance, and effective radius over the 0.1–1-μm radius range under humidified ambient conditions with 500-m vertical resolution and uncertainties of 100%, 50%, and 10%, respectively. Shallow, broken marine clouds provide an example of conditions where boundary layer aerosol properties would be retrieved in clear-sky gaps. To quantify the degree of constraint that proposed retrievals might provide on cloud radiative forcing (CRF) simulated by climate models under such conditions, dry aerosol size distribution parameters are independently varied here in large-eddy simulations of three well-established modeling case studies. Using the rudimentary available aerosol specifications, it is found that relative changes of total dry aerosol properties in simulations can be used as a proxy for relative changes of ambient aerosol properties targeted by ACE retrievals. The sensitivity of simulated daytime shortwave CRF to the proposed uncertainty in retrieved aerosol number concentration is -15 W m^{-2} in the overcast limit, roughly a factor of 2 smaller than a simple analytic estimate owing primarily to aerosol-induced reductions in simulated liquid water path across this particular set of case studies. The CRF sensitivity to proposed uncertainties in retrieved aerosol effective variance and effective radius is typically far smaller, with no corresponding analytic estimate. Generalization of the results obtained here using only three case studies would require statistical analysis of relevant meteorological and aerosol observations and quantification of observational and model uncertainties and biases.

1. Introduction

The interactions of aerosols with clouds represent a leading source of uncertainty in quantifying anthropogenic radiative forcing of climate globally since preindustrial times (Solomon et al. 2007). Clouds are also reported to constitute the largest source of uncertainty in climate sensitivity to radiative forcing in current coupled ocean–atmosphere climate models (Soden and Held 2006). In the tropics, differences in the predicted sensitivity of marine boundary layer clouds to CO_2 doubling have been specifically identified as the main source of uncertainty in cloud feedback (Bony and Dufresne 2005).

The contribution of low cloud properties to both anthropogenic radiative forcing of climate and climate sensitivity has motivated extensive efforts to characterize the interactions of aerosols with low clouds and improve their representation in climate models. Whereas in situ measurements are generally most capable of characterizing localized aerosol and cloud microphysical properties in detail, routine satellite-based measurements provide long-term global coverage that is useful for constraining climate models (e.g., Quaas et al. 2009). However, a common disadvantage of satellite retrievals relative to other measurements is reduced spatial resolution and measurement sensitivity. The process of determining whether specific proposed retrievals will be adequate to meet intended scientific needs is therefore critical.

In a recent U.S. decadal survey for Earth observations from space (National Research Council 2007), objectives for the National Aeronautics and Space Administration (NASA) Aerosol–Clouds–Ecosystem (ACE) satellite mission include retrieval of aerosol and cloud property profiles. Here we focus on the proposed retrieval of the number, effective variance, and effective radius of ambient aerosols in the 0.1–1-μm radius range at 500-m

Corresponding author address: Ann Fridlind, 2880 Broadway, NASA Goddard Institute for Space Studies, New York, NY 10025. E-mail: ann.fridlind@nasa.gov

DOI: 10.1175/2010JTECHA1520.1

vertical resolution with associated uncertainties of 100%, 50%, and 10%, respectively. These definitions represent nominal aerosol retrieval requirements established during ACE mission planning, which are intended for the purpose of better constraining the representation of aerosol–cloud interactions in climate models, to be distinguished from the proposed requirements for the retrieval of other aerosol properties more closely tied to the direct effects of aerosols on the atmospheric radiative budget. The retrieval of ambient rather than dry aerosol size distribution properties is considered to reduce the dependence of retrieval accuracy on collocated atmospheric state profiles that are not measured by the ACE mission (such as relative humidity) and size-resolved aerosol composition.

Given the proposed ACE uncertainty requirements placed on the retrieval of these and other aerosol and cloud property profiles, ACE mission planning efforts aim to systematically estimate relevant associated uncertainties in top-of-atmosphere radiative forcing as a common metric for considering the adequacy of each retrieval to meet intended scientific needs. It is our objective here to use large-eddy simulations with resolved aerosol and cloud particle size distributions to estimate the top-of-atmosphere cloud radiative forcing (CRF) associated with the specific proposed aerosol parameter uncertainties described above. We focus on broken low clouds in order to evaluate the sensitivity of cloud properties to aerosol properties below the cloud base, which are observable in cloud-free pixels among cloudy pixels by virtue of boundary layer mixing. We consider only marine clouds to limit the number of surface parameters. We treat all of the aerosol as ammonium bisulfate to limit the number of aerosol composition parameters. The objective is to estimate aggregate CRF sensitivity to proposed retrieval uncertainties, including, but not limited to, any induced changes in cloud albedo, cover, and thickness.

We emphasize that quantifying the potential radiative impact of anthropogenic aerosols on broken marine cloud fields is not an objective of this work. Rather, we aim only to quantify CRF sensitivity to proposed uncertainties in retrievals of specific aerosol properties. The general application in mind here is not the observational correlation of aerosol with cloud properties, but rather the constraint of aerosol properties beneath broken cloud fields in climate models, which is considered in terms of associated CRF at the local scale (over individual broken cloud fields) and at the global scale (considering the global frequency and variety of broken cloud fields). For example, what is the possible CRF uncertainty associated with an uncertainty of 50% in the effective variance of aerosols in the 0.1–1-μm size range averaged over a 500-m layer at ambient relative humidity beneath a broken marine cloud field?

We are aware of no literature that quantifies the sensitivity of CRF over broken marine clouds to the specific aerosol properties targeted by ACE. There are two main barriers to adapting past work to meet the needs of this study. First, the aerosol properties targeted by ACE retrievals cannot be universally related to commonly considered aerosol properties, such as the total concentration of cloud condensation nuclei (CCN; e.g., McComiskey and Feingold 2008). CCN as a function of supersaturation is calculated during the course of the simulations here, but the inverse derivation of ACE aerosol size distribution properties from CCN requires the specification of detailed underlying aerosol and meteorological conditions. Second, observationally based studies generally rely upon the categorizing of observed conditions in terms of meteorological and cloud properties in order to isolate aerosol influences (e.g., Garrett and Zhao 2006), whereas the objective of the calculations presented here is to calculate the total CRF sensitivity to aerosol retrieval uncertainties, including the dynamical response, which cannot be assumed to be negligible (e.g., Garrett et al. 2009).

2. Simulations

The three cases of shallow, broken marine clouds developed for model intercomparison studies organized by the Global Energy and Water Cycle Experiment (GEWEX) Cloud System Study (GCSS) program are used as the basis for this study. We are aware of no other well-established modeling case studies. The cases are representative of trade wind cumuli observed during the Atlantic Trade Wind Experiment (ATEX; Stevens et al. 2001), the Barbados Oceanographic and Meteorological Experiment (BOMEX; Siebesma et al. 2003), and the Rain in Cumulus over Ocean (RICO) experiment (van Zanten et al. 2011).

Simulations are performed with the Distributed Hydrodynamic–Aerosol–Radiation Modeling Application (DHARMA; Stevens et al. 2002; Ackerman et al. 2004), a large-eddy simulation code coupled with size-resolved microphysics based on the Community Aerosol–Radiation–Microphysics for Atmospheres (CARMA) code (Ackerman et al. 1995; Jensen et al. 1998). Initial conditions and forcings follow the model intercomparison specifications for each case. The ATEX, BOMEX, and RICO simulations use uniform horizontal and vertical grid spacing of 100 and 40 m over a domain of 9.6 km $\times$ 9.6 km $\times$ 3 km (ATEX and BOMEX) or 12.8 km $\times$ 12.8 km $\times$ 4 km (RICO), a mass-doubling particle grid of 25 bins (ATEX and BOMEX) or 35 bins (RICO), and

TABLE 1. Aerosol size distribution parameters in the 0.1–1-μm radius range under dry and ambient conditions. For a single lognormal mode over all sizes, $\nu_e = \exp(\ln^2\sigma_g) - 1$ and $r_e = r_g \exp[(5/2)\ln^2\sigma_g]$. For more than one mode or a limited radius range, $\nu_e = \int(r - r_e)^2 r^2 N(r)\, dr / \int r_e^2 r^2 N(r)\, dr$ and $r_e = \int r^3 N(r)\, dr / \int r^2 N(r)\, dr$.

Case	Dry total ν_e (−)	Dry 0.1–1-μm ν_e (−)	Ambient 0.1–1-μm ν_e (−)	Dry total r_e (μm)	Dry 0.1–1-μm r_e (μm)	Ambient 0.1–1-μm r_e (μm)
ATEX baseline	0.18	0.13	0.17	0.15	0.16	0.20
ATEX narrow	0.09	0.06	0.09	0.12	0.13	0.16
BOMEX baseline	0.18	0.13	0.18	0.15	0.16	0.22
BOMEX narrow	0.09	0.06	0.10	0.12	0.13	0.18
RICO baseline	0.54	0.27	0.23	0.27	0.30	0.39
RICO narrow	0.27	0.10	0.12	0.15	0.18	0.25

a duration of 6–8 h. Radiative cooling follows intercomparison specifications, in which a horizontally uniform cooling rate is used for BOMEX and RICO simulations (cloud cover is less than 10%) and a Beer's law parameterization of longwave cooling that depends on the condensed water profile in each column is used for ATEX. When offline shortwave radiative flux calculations are made, a solar zenith angle (θ) of 60° and a solar constant (S_o) of 1367 W m^{-2} are used.

The only inputs that vary across simulations of each case are aerosol size distribution parameters, which are initialized uniformly throughout the domain. A diagnostic approach (Clark 1974) is used to avoid the need to specify unknown aerosol source terms and track core second moments (to restore aerosol dispersion upon droplet evaporation). For the ATEX and BOMEX cases, aerosols are assumed to be present in a single lognormal mode with baseline dry number concentration (N_a) of 75 cm^{-3}, a geometric mean radius (r_g) of 0.1 μm, and a geometric standard deviation (σ_g) of 1.5; in terms of the aerosol uncertainties considered here for satellite remote sensing, dry effective radius (r_e) is 0.15 μm and effective variance (ν_e), as defined by Nakajima and King (1990), is 0.18. These size distribution properties are chosen to be generally representative of marine conditions. For the RICO case, based on available case-specific measurements used in the model intercomparison, baseline bimodal lognormal dry aerosol parameters are N_a = 90 and 15 cm^{-3}, with r_g = 0.03 and 0.14 μm and σ_g = 1.28 and 1.75, respectively; for the total population dry r_e = 0.27 μm and ν_e = 0.54. Ambient aerosol sizes are calculated assuming equilibrium with grid-scale relative humidity as described in Charlson et al. (2007).

Two types of sensitivity tests are carried out for ATEX, BOMEX, and RICO: (i) N_a is progressively doubled 2 or 3 times, and (ii) ν_e is reduced by 50% once for each N_a. The latter is accomplished by reducing σ_g to 1.34 for the ATEX and BOMEX cases and by reducing σ_g of the larger mode to 1.37 for the RICO case. Decreases in ν_e, like increases in N_a, induce increases in activated droplet number concentration. Because ν_e reductions of 50% result in r_e decreases of more than 10% (see dry total values in Table 1), we omit separate simulations for 10% changes in r_e. Aside, we note that r_e decreases achieved by reducing r_g (rather than decreasing ν_e) decrease rather than increase activated droplet number concentration, but we find that the relative absolute magnitude of response is comparable in a typical simulation (not shown) and is far weaker than the response to uncertainty in number concentration, as described below.

3. Results

After model spinup (1–2 h), domain-averaged droplet number concentration is relatively constant in all simulations, but liquid water path (LWP) and cloud cover may evolve, depending upon the case. Figure 1 illustrates the cloud state at the end of each baseline simulation.

We first consider the possible relationship of satellite-observable near-surface aerosol properties, which are viewable between broken clouds under ambient relative humidity conditions, to the dry aerosol properties carried in large-eddy simulation (LES) and climate models. Using the last four 3D output fields saved from each simulation (spanning the last 1.5 h of each simulation), we average aerosol number concentration in the 0.1–1-μm radius range over grid cells below 500 m in clear columns, defined as those where mid-visible optical thickness (τ, including cloud, haze, and gases) is less than 2.5 (using a threshold of 1.0 changes results negligibly). Figure 2 illustrates the results for three representative simulations. In the ATEX cases (monomodal aerosol), more aerosols are present in the 0.1–1-μm radius range under ambient versus dry conditions because hydration leads to growth into that size range. In the RICO case (bimodal aerosol), aerosol concentration in the 0.1–1-μm radius range is roughly identical under ambient versus dry conditions because the larger aerosol mode is already mostly in that radius range when dry.

For all cases, the doublings of the aerosol number in the 0.1–1-μm radius range under clear-sky ambient

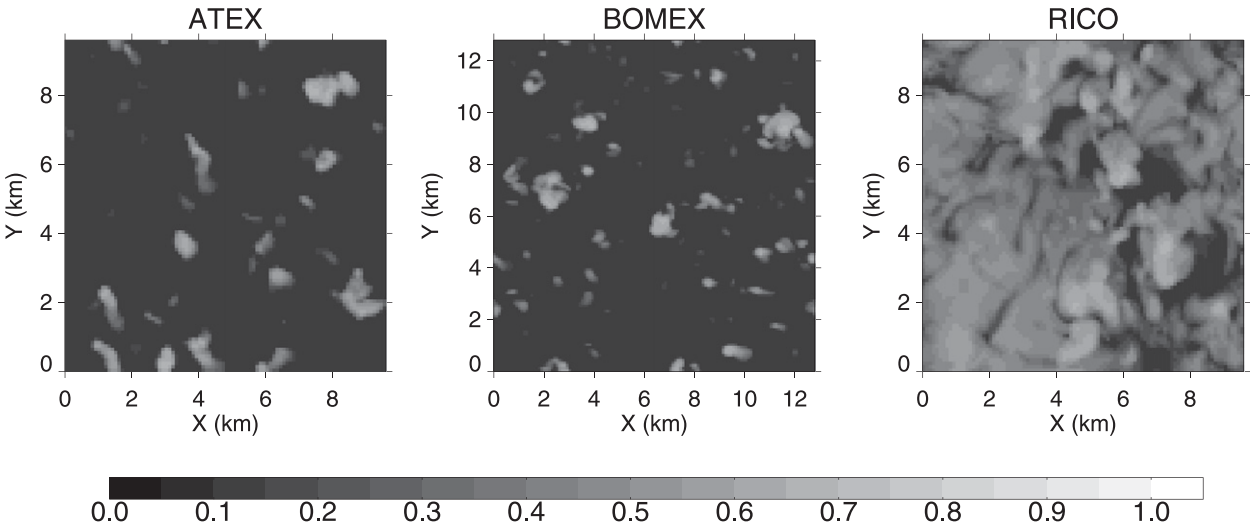

FIG. 1. Top-of-atmosphere albedo at the end of the simulation with the lowest aerosol number concentration and baseline effective variance for each case.

conditions (the quantity targeted by satellite retrievals) correspond directly to the doublings of total dry N_a (the more fundamental underlying quantity). Results for ν_e and r_e (summarized in Table 1) indicate a similar correspondence of relative changes in ambient clear-sky near-surface values in the 0.1–1-μm radius range with relative changes in dry all-sky values. Thus, for the purposes of this study, sensitivity to relative changes of total dry aerosol properties can be adopted as a proxy for sensitivity to relative changes of ambient humidified aerosol properties targeted by ACE retrievals. It is unknown to what degree this would be true under naturally varying aerosol conditions, as discussed further below.

We turn next to CRF. Because the simulated response of broken cloud fields to N_a changes can be small compared to internal variability (e.g., Xue and Feingold 2006; Xue et al. 2008), we employ the following run-time approximation of shortwave daytime CRF that does not rely on less frequent offline radiative calculations:

$$\mathrm{CRF} = -kS_o \cos(\theta) A = -kS_o \cos(\theta) f_c \frac{\tau_c}{\tau_c + 13} \quad (1)$$

[Ramanathan 1987; his Eq. (14) with a clear-sky albedo of 0], where the ratio of top-of-the-atmosphere (TOA) broadband to cloud-top mid-visible albedo (k) is assumed to be 0.8 (Charlson et al. 1992) and the domain-averaged mid-visible albedo at cloud top (A) is approximated as the fractional cloud cover (f_c) multiplied by a cloudy-sky albedo of $\tau_c/(\tau_c + 13)$ [Bohren 1987; his Eq. (14) with an asymmetry parameter of 0.85], where τ_c is defined as the optical thickness of activated droplets treated as geometric scatterers (twice the total droplet cross-sectional area). By computing an albedo for the cloudy portion of the model domain from τ_c averaged over the cloudy columns,[1] we ignore any variability among the cloudy columns, analogous to the partly cloudy retrieval scheme of Coakley et al. (2005). By only differentiating between clear and cloudy columns such an approach does not fully address the plane-parallel albedo bias (Cahalan et al. 1994). However, the scene albedo thus computed on average is within 0.01 (relative errors within 10%) of that using the independent column approximation.

Figure 3 illustrates the CRF calculated for sequential doublings of aerosol number concentration using the baseline and 50% reduced ν_e values in all cases. Also shown are the domain-averaged droplet number concentration (weighted by the mass mixing ratio of condensed water, N_d), LWP, and cloud cover. In the ATEX case, LWP decreases can be substantial despite increases in cloud cover, consistent with other ATEX and BOMEX studies (Xue and Feingold 2006; Xue et al. 2008).[2] Relative changes in N_d induced by reducing ν_e are always far less than those induced by doubling N_a. Reducing ν_e allows the smallest aerosols to be more easily activated, consistent with the modest N_d increases

[1] Defined as those with $\tau_c > 2.5$ through the rest of our analysis.

[2] Owing to the complexity of the interactions between microphysics, radiation, and dynamics over a wide range of aerosol and precipitation conditions across three different cases here, it is beyond the scope of this study to attribute changes in various simulation diagnostics to specific mechanisms. However, it is reasonable to expect that behavior similar to that found in past studies using a similar modeling framework can be attributed to similar causes.

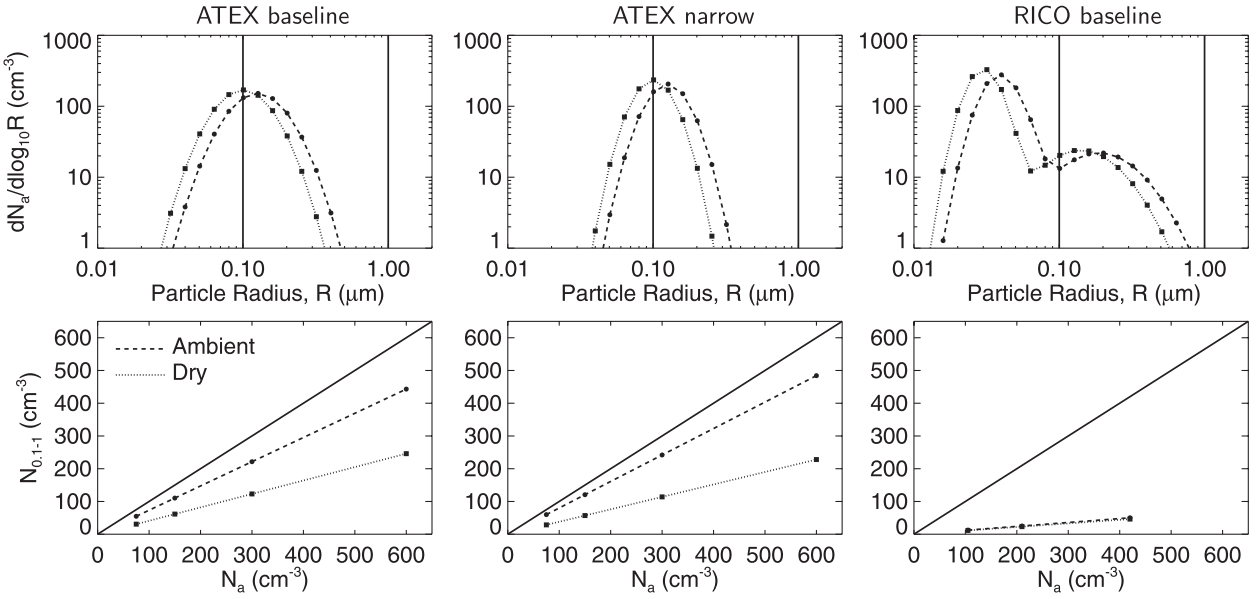

FIG. 2. For (left to right) ATEX baseline, ATEX narrow, and RICO baseline representative simulations: average aerosol number size distribution in the lowermost 500 m of cloud-free columns at simulated ambient humidity (dashed) and when dry (dotted) for (top) the smallest values in aerosol number concentration (N_a) progressions (solid lines indicate limits of 0.1–1-μm radius range), and (bottom) number concentrations in the 0.1–1-μm radius range vs total N_a for progressive doublings (solid line is 1:1).

induced by decreasing ν_e for ATEX and BOMEX; the maximum response of N_d to reducing ν_e is about 10% of that induced by doubling N_a. For RICO, all aerosols in the larger mode are activated regardless of ν_e. In both cases, increased N_d results in modestly decreased peak supersaturations (not shown), and N_d thus increases somewhat less than linearly with N_a in both cases.

The change in TOA cloud radiative forcing (ΔCRF), the final metric for this study, is shown in Fig. 4. Over this handful of cases, the ΔCRF response to progressive doublings of N_a is similar for the baseline and reduced (narrow) ν_e values, and the sensitivity to halving ν_e (equivalent to greater than 10% change in r_e) is typically far smaller in absolute magnitude. For changes induced by doubling N_a, ΔCRF tends to strengthen with increasing N_a.

Aggregating over all cases, ΔCRF is seen in Fig. 5 to generally strengthen with increasing cloud cover, indicating that relative changes in cloud cover within each case are smaller than relative changes in cloud albedo. Also shown in Fig. 5 is an analytic estimate for the daytime Twomey effect induced by a doubling of N_a for overcast conditions over a nonreflecting surface, assuming constant liquid water path and a constant relative dispersion of droplet size distributions,

$$\Delta\mathrm{CRF} = -kS_o\cos(\theta)\Delta A = -kS_o\cos(\theta)\frac{A(1-A)}{3}\Delta\ln N_a, \quad (2)$$

where we equate relative changes in N_d with those in N_a ($\Delta\ln N_d = \Delta\ln N_d = \ln 2$) and approximate $\Delta A/\Delta\ln N_d$ from the maximum value of $dA/d\ln N_d = A(1 - A)/3$ at $A = 0.5$ (Twomey 1991). A linear least squares fit through the broken cloud cases simulated here (ATEX, BOMEX, and RICO) gives an intercept near 0 and intersects the overcast limit at roughly -15 W m^{-2}. The factor-of-2 difference between that and the roughly -30 W m^{-2} obtained from Eq. (2) indicates that offsets to the Twomey effect from simulated reductions in LWP are substantial across these three well-established broken cloud cases. We emphasize that these three cases cannot be expected to be representative of a meaningful climatology, as discussed further below. In Fig. 5, the wide range of ΔCRF calculated from three overcast stratocumulus cases simulated by Ackerman et al. (2004) is representative of cases in which aerosol-induced changes in LWP are both positive and negative. It is unknown to what degree positive liquid water path changes would contribute to the climatology of broken cloud cases. The linear fit through the broken cloud cases presented here is seen to run through the weak end of the range of ΔCRF calculated for stratocumulus cases, and much stronger (more negative) ΔCRF is shown for other stratocumulus cases in which LWP increases with N_a (see Ackerman et al. 2004).

Based on the results of the broken cloud cases in hand, however, we now briefly consider what global CRF uncertainty could be associated with uncertainties in

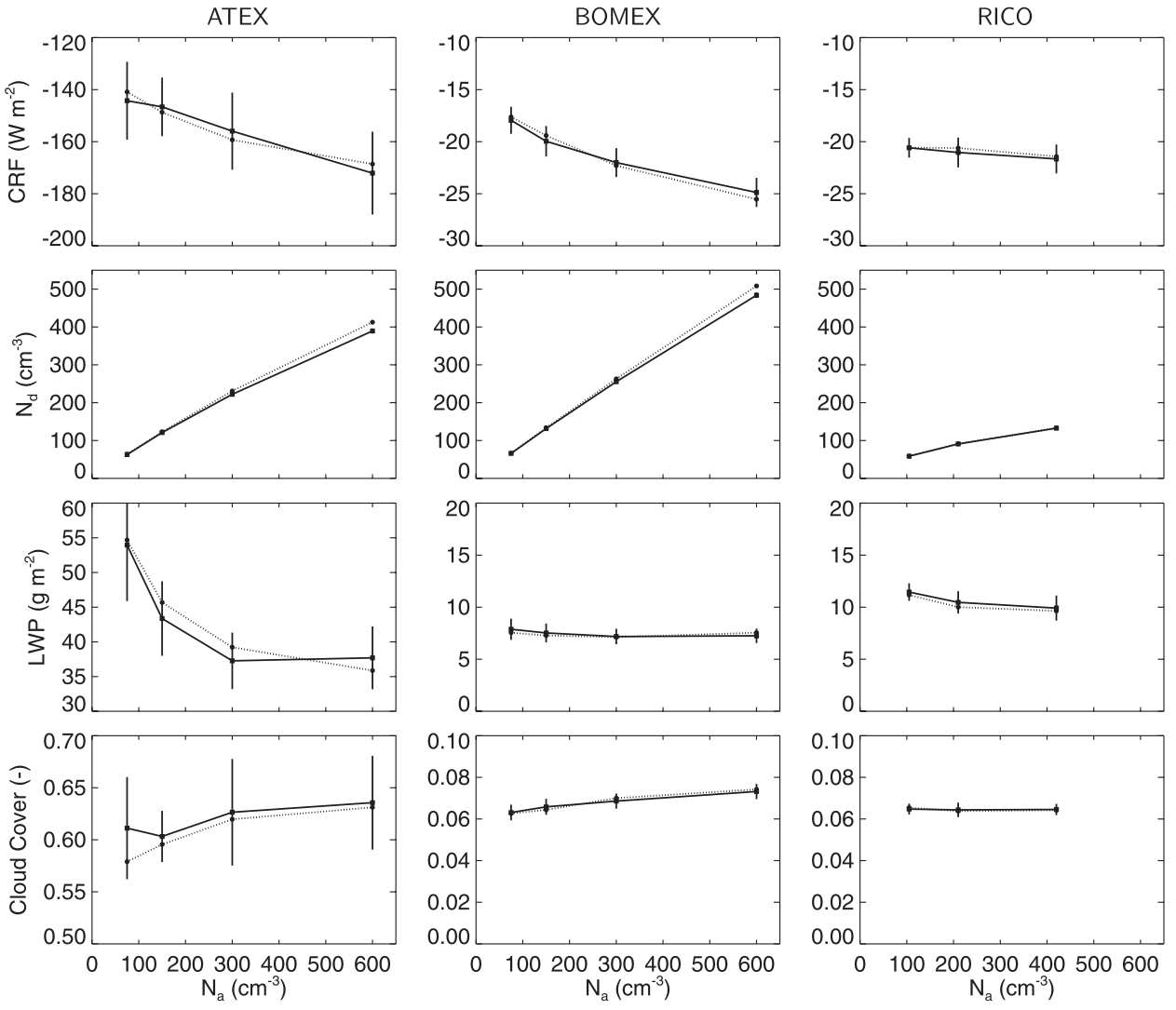

FIG. 3. For (left to right) ATEX, BOMEX, and RICO simulations with progressive doublings of N_a: (top to bottom) shortwave daytime CRF, N_d, LWP, and cloud cover vs total N_a using the baseline ν_e (solid lines) and 50% reduced ν_e (dotted lines). All values are averages of 1-min domain means over the last 4 h of simulations. Error bars (shown only for baseline ν_e) represent a standard deviation of contributing values and include the effect of any underlying trends.

proposed retrieved aerosol properties. Broken marine cloud fields may be uniquely germane for the constraint of climate model representation of aerosol effects on cloud properties using satellite retrievals since warm low-level clouds are considered to be susceptible to aerosol influences (as discussed in section 1), the observable aerosols are relevant to the collocated clouds (which may not be the case for overcast stratocumulus, e.g.), and underlying marine surfaces provide superior retrieval conditions. Of the retrieval uncertainties considered here, the ΔCRF associated with N_a uncertainty is the largest and therefore would dominate. The mean frequency of cumulus from surface observations is reported as 34% over global oceans, with a mean cloud cover of 38% when present (Warren et al. 1988), which is represented by the dashed line in Fig. 5. Intersection with the linear fit at roughly -6 W m^{-2} provides a global equivalent uncertainty in diurnal shortwave CRF of roughly 0.7 W m^{-2}, which is arrived at by multiplying 6 W m^{-2} by the mean global frequency of 0.34, the fraction of the earth surface covered by ocean of 0.7, and a fraction of 0.5 to account for the fraction of the globe that is illuminated. Thus, in a simplistically considered global model, if the number concentration of 0.1–1-μm near-surface aerosols at ambient relative humidity representative of clear-sky conditions in broken marine clouds fields were 100% greater than perfectly known values, simulated global CRF could diverge by at least 0.7 W m^{-2} from a correct

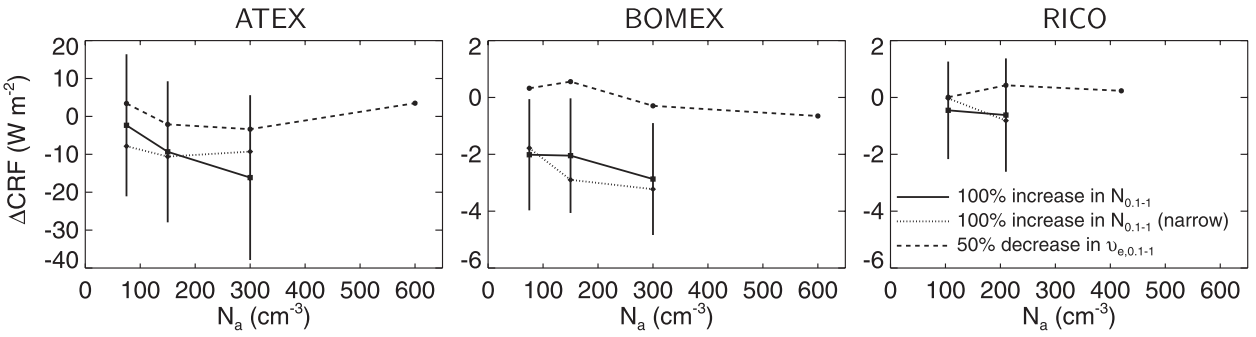

FIG. 4. For (left to right) ATEX, BOMEX, and RICO change in shortwave daytime CRF induced by progressive doublings of N_a at baseline ν_e (solid lines) and at 50% reduced ν_e (dotted lines; "narrow"), and by 50% reduction of ν_e at a given N_a (dashed lines).

value. This is a lower limit to uncertainty in part because it assumes that the relationship of the retrieved aerosol property to the total dry aerosol size distribution is also known, but it serves to quantitatively illustrate the degree to which uncertainties in currently proposed aerosol property retrievals may be associated with limitations in their ability to constrain global CRF in climate model results with respect to one relevant cloud type.

Generalizing this study regionally or climatologically would require statistical evaluation of the relevant meteorological and aerosol conditions and synthesis of an appropriately representative ensemble of case studies, in addition to quantification of uncertainties and biases, which cannot be assumed to be insignificant for either the models (e.g., Stevens and Seifert 2008) or observations (e.g., obtaining statistically representative coverage diurnally and regionally).

4. Summary and discussion

NASA's ACE satellite mission proposes to retrieve vertical profiles of aerosol number concentration, effective variance, and effective radius over the 0.1–1-μm radius range under humidified ambient conditions with 500-m vertical resolution and uncertainties of 100%, 50%, and 10%, respectively. Shallow, broken marine clouds provide an example of conditions where boundary layer aerosol properties would be retrieved in clear-sky columns. The degree to which proposed aerosol profile retrievals would contribute to constraining climate model representation of top-of-atmosphere cloud radiative forcing (CRF) under such conditions is quantified using large-eddy simulations of three well-established model intercomparison case studies.

For the rudimentary aerosol representations in each case, it is first found that relative changes in total dry aerosol properties can be used as a proxy for relative changes in ambient aerosol properties targeted by ACE retrievals. Namely, the fraction of humidified aerosol in the 0.1–1-μm radius range at 0–500 m in clear columns doubles along with total aerosol number concentration (N_a). Similarly, the clear-sky ambient aerosol effective variance (ν_e) in the 0.1–1-μm radius range is roughly halved along with a 50% reduction in dry ν_e, and corresponds to greater than 10% changes in either dry or clear-sky ambient effective radius (r_e, see Table 1).

The sensitivity of daytime shortwave CRF to the proposed 100% uncertainty in retrieved aerosol number concentration is found to be -15 W m^{-2} in the overcast limit. This is roughly a factor of 2 smaller in magnitude than an analytic estimate of the Twomey effect owing primarily to aerosol-induced reductions in liquid water path across the small set of case studies considered here. It is unknown to what degree aerosol-induced increases in

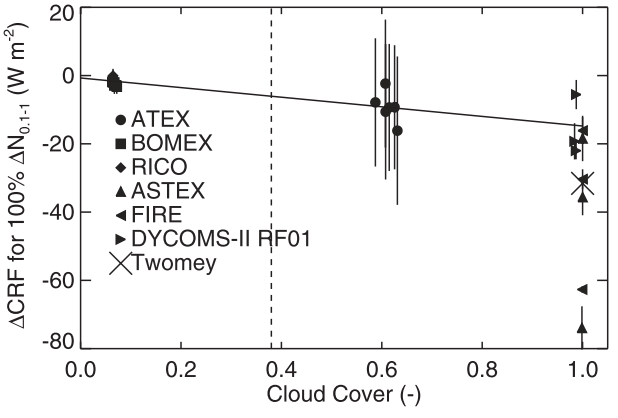

FIG. 5. The ΔCRF from doubling N_a vs cloud cover for all cases. A least squares linear fit through ATEX, BOMEX, and RICO cases has an intercept of -0.7 W m^{-2} and a slope of -15 W m^{-2}. An analytic estimate of the Twomey effect [Eq. (2)] gives a value of -33 W m^{-2} for overcast conditions. By comparison, simulations of stratocumulus (Ackerman et al. 2004) give values from -6 to -73 W m^{-2} in the overcast limit. Cloud cover of 0.38 (dashed line) is global mean over oceans when cumulus is present based on surface observations compiled by Warren et al. (1988).

liquid water path, demonstrated to occur for overcast stratocumulus (e.g., Ackerman et al. 2004), would contribute to a climatology of broken cloud cases, thereby increasing CRF sensitivity. In the three cases considered here, CRF sensitivity to the proposed uncertainty of 50% in retrieved ν_e (equivalent to changing retrieved r_e by more than the proposed uncertainty of 10%) is typically far weaker than the sensitivity to proposed uncertainty in retrieved aerosol number concentration. These results are intended to aid in the evaluation of the proposed ACE aerosol retrieval requirements.

A notable aspect of these case studies is the large difference between the bimodal aerosol size distribution shape for the RICO case and the monomodal shape for the other cases. As a consequence of the shape difference, the number of aerosols in the 0.1–1-μm radius range is a small fraction of those serving as cloud condensation nuclei in the RICO case and exceeds 25 cm^{-3} only at the highest N_a value considered (see Fig. 2). Such low concentrations near the surface could be challenging to detect via satellite. In addition, we have assumed that aerosol numbers in the accumulation mode are perfectly correlated with aerosol numbers in the Aitken mode, but no such correlation is guaranteed in nature. The lack of such correlation would prevent the use of relative changes in humidified aerosol properties in a limited radius range as a reliable proxy for relative changes in total dry aerosol properties, for instance. Thus, to obtain regionally applicable results, the climatology of aerosol number size distribution parameters may be at least as important as thermodynamic conditions, and their covariability may also be important. Finally, although our assumption of ammonium bisulfate aerosol composition is expected to provide a reasonably accurate representation of aerosol activation properties under a relatively wide range of natural conditions (e.g., VanReken et al. 2003), and the variability of composition is expected to be of secondary importance compared with the variability of aerosol number size distribution properties (e.g., Dusek et al. 2006), the covarying climatology of size-distributed aerosol composition may also be important.

Acknowledgments. Financial and computational support was provided by the NASA Radiation Sciences Program and the NASA Advanced Supercomputing Division. We thank three anonymous reviewers and the authors of NASA's ACE white papers for useful comments. We thank Alexander Avramov for contributions to model analysis.

REFERENCES

Ackerman, A. S., P. V. Hobbs, and O. B. Toon, 1995: A model for particle microphysics, turbulent mixing, and radiative transfer in the stratocumulus-topped marine boundary layer and comparisons with measurements. *J. Atmos. Sci.,* **52,** 1204–1236.

——, M. P. Kirkpatrick, D. E. Stevens, and O. B. Toon, 2004: The impact of humidity above stratiform clouds on indirect aerosol climate forcing. *Nature,* **432,** 1014–1017.

Bohren, C. F., 1987: Multiple scattering of light and some of its observable consequences. *Amer. J. Phys.,* **55,** 524–533.

Bony, S., and J.-L. Dufresne, 2005: Marine boundary layer clouds at the heart of tropical cloud feedback uncertainties in climate models. *Geophys. Res. Lett.,* **32,** L20806, doi:10.1029/2005GL023851.

Cahalan, R. F., W. Ridgway, W. J. Wiscombe, T. L. Bell, and J. B. Snider, 1994: The albedo of fractal stratocumulus clouds. *J. Atmos. Sci.,* **51,** 2434–2455.

Charlson, R. J., S. E. Schwartz, J. M. Hales, R. D. Cess, J. A. Coakley, J. E. Hansen, and D. J. Hofmann, 1992: Climate forcing by anthropogenic aerosols. *Science,* **255,** 423–430.

——, A. S. Ackerman, F. A. M. Bender, T. L. Anderson, and Z. Liu, 2007: On the climate forcing consequences of the albedo continuum between cloudy and clear air. *Tellus,* **59B,** 715–727.

Clark, T. L., 1974: A study in cloud phase parameterization using the gamma distribution. *J. Atmos. Sci.,* **31,** 142–155.

Coakley, J. A., M. A. Friedman, and W. R. Tahnk, 2005: Retrieval of cloud properties for partly cloudy imager pixels. *J. Atmos. Oceanic Technol.,* **22,** 3–17.

Dusek, U., and Coauthors, 2006: Size matters more than chemistry for cloud-nucleating ability of aerosol particles. *Science,* **312,** 1375–1378.

Garrett, T. J., and C. Zhao, 2006: Increased Arctic cloud longwave emissivity associated with pollution from mid-latitudes. *Nature,* **440,** 787–789.

——, M. M. Maestas, S. K. Krueger, and C. T. Schmidt, 2009: Acceleration by aerosol of a radiative-thermodynamic cloud feedback influencing Arctic surface warming. *Geophys. Res. Lett.,* **36,** L19804, doi:10.1029/2009GL040195.

Jensen, E. J., and Coauthors, 1998: Ice nucleation processes in upper tropospheric wave-clouds observed during SUCCESS. *Geophys. Res. Lett.,* **25,** 1363–1366.

McComiskey, A., and G. Feingold, 2008: Quantifying error in the radiative forcing of the first aerosol indirect effect. *Geophys. Res. Lett.,* **35,** L02810, doi:10.1029/2007GL032667.

Nakajima, T., and M. D. King, 1990: Determination of the optical thickness and effective particle radius of clouds from reflected solar radiation measurements. Part I: Theory. *J. Atmos. Sci.,* **47,** 1878–1893.

National Research Council, 2007: *Earth Science and Applications from Space: National Imperatives for the Next Decade and Beyond*. The National Academies Press, 428 pp.

Quaas, J., and Coauthors, 2009: Aerosol indirect effects–general circulation model intercomparison and evaluation with satellite data. *Atmos. Chem. Phys.,* **9,** 12 731–12 779.

Ramanathan, V., 1987: The role of earth radiation budget studies in climate and general circulation research. *J. Geophys. Res.,* **92** (D4), 4075–4095.

Siebesma, A. P., and Coauthors, 2003: A large eddy simulation intercomparison study of shallow cumulus convection. *J. Atmos. Sci.,* **60,** 1201–1219.

Soden, B. J., and I. M. Held, 2006: An assessment of climate feedbacks in coupled ocean–atmosphere models. *J. Climate,* **19,** 3354–3360.

Solomon, S., D. Qin, M. Manning, M. Marquis, K. Averyt, M. M. B. Tignor, H. L. Miller Jr., and Z. Chen, Eds., 2007:

Climate Change 2007: The Physical Science Basis. Cambridge University Press, 996 pp.

Stevens, B., and A. Seifert, 2008: Understanding macrophysical outcomes of microphysical choices in simulations of shallow cumulus convection. *J. Meteor. Soc. Japan,* **86,** 143–162.

——, and Coauthors, 2001: Simulations of trade wind cumuli under a strong inversion. *J. Atmos. Sci.,* **58,** 1870–1891.

Stevens, D. E., A. S. Ackerman, and C. S. Bretherton, 2002: Effects of domain size and numerical resolution on the simulation of shallow cumulus convection. *J. Atmos. Sci.,* **59** (23), 3285–3301.

Twomey, S., 1991: Aerosols, clouds and radiation. *Atmos. Environ.,* **25A** (11), 2435–2442.

VanReken, T. M., T. A. Rissman, G. C. Roberts, V. Varutbangkul, H. H. Jonsson, R. C. Flagan, and J. H. Seinfeld, 2003: Toward aerosol/cloud condensation nuclei (CCN) closure during CRYSTAL-FACE. *J. Geophys. Res.,* **108,** 4633, doi:10.1029/2003JD003582.

van Zanten, M. C., and Coauthors, 2011: Controls on precipitation and cloudiness in simulations of trade-wind cumulus as observed during RICO. *J. Adv. Model. Earth Syst.,* in press.

Warren, S. G., C. J. Hahn, J. London, R. M. Chervin, and R. L. Jenne, 1988: Global distribution of total cloud cover and cloud type amounts over the ocean. U.S. DOE Office of Energy Research Tech. Rep. DOE/ER-0406, 212 pp.

Xue, H., and G. Feingold, 2006: Large-eddy simulations of trade wind cumuli: Investigation of aerosol indirect effects. *J. Atmos. Sci.,* **63,** 1605–1622.

——, ——, and B. Stevens, 2008: Aerosol effects on clouds, precipitation, and the organization of shallow cumulus convection. *J. Atmos. Sci.,* **65,** 392–406.

CORRIGENDUM

ANN M. FRIDLIND AND ANDREW S. ACKERMAN

NASA Goddard Institute for Space Studies, New York, New York

(Manuscript received and in final form 19 May 2011)

In Fridlind and Ackerman (2011) we mislabeled the panels of Fig. 1. A corrected Fig. 1 is shown below.

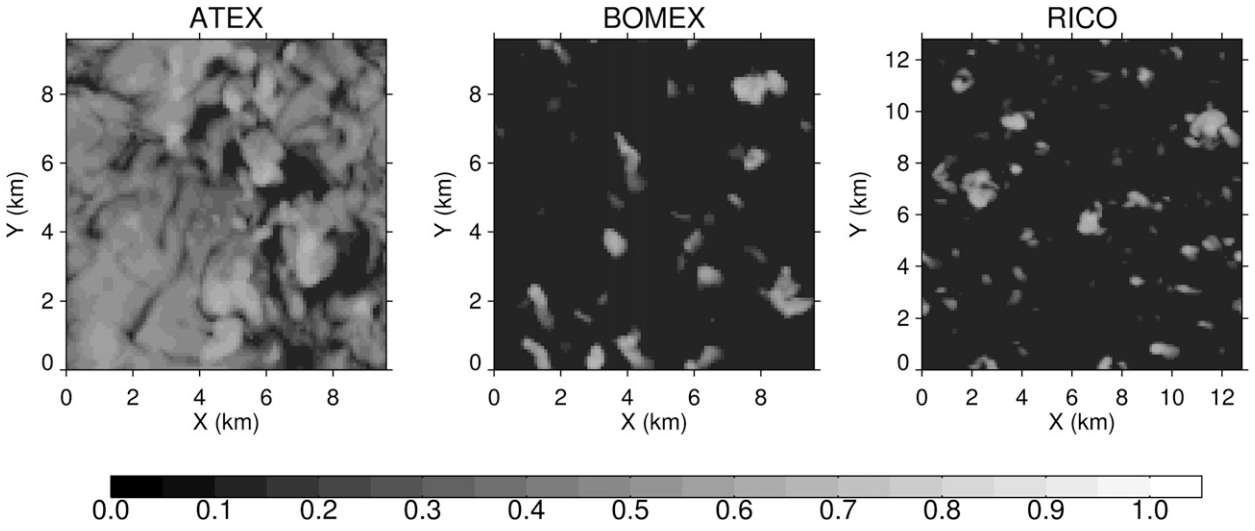

FIG. 1. Top-of-atmosphere albedo at the end of the simulation with the lowest aerosol number concentration and baseline effective variance for each case.

REFERENCE

Fridlind, A., and A. S. Ackerman, 2011: Estimating the sensitivity of radiative impacts of shallow, broken marine clouds to boundary layer aerosol size distribution parameter uncertainties for evaluation of satellite retrieval requirements. *J. Atmos. Oceanic Technol.,* **28,** 530–538.

Corresponding author address: Ann Fridlind, 2880 Broadway, NASA Goddard Institute for Space Studies, New York, NY 10025.
E-mail: ann.fridlind@nasa.gov

DOI: 10.1175/JTECH-D-11-00098.1